

# Coded Aperture Design by Motion Estimation Using Sparse Representation in Adaptive Compressed Spectral Video Sensing

PhD(c) N. Diaz<sup>1</sup>, MS(c) C. Noriega <sup>1</sup>  
Ph.D A. Basarab <sup>3</sup>, Ph.D J-Y. Tourneret <sup>3</sup>  
Advisor: Ph.D H. Arguello <sup>2</sup>

<sup>1</sup>Department of Electrical and Computer Engineering,

<sup>2</sup>Department of Computer Science

Universidad Industrial de Santander, Bucaramanga, Colombia.

<sup>3</sup>University of Toulouse, Toulouse, Francia.

March 5, 2022



# Outline

## 1 Introduction

- Challenges in Video-CSI

## 2 Methods

- Motion Estimation in Spectral Imaging
- Sparse regularization term
- Dictionary Filters and Coefficient Maps
- Adaptive Video Colored Coded Aperture Design

## 3 Results

- Simulation Parameters
- Quality of Image Reconstruction

## 4 Conclusions

- Video Motion Estimation Algorithm

# Challenges in Video-CSI

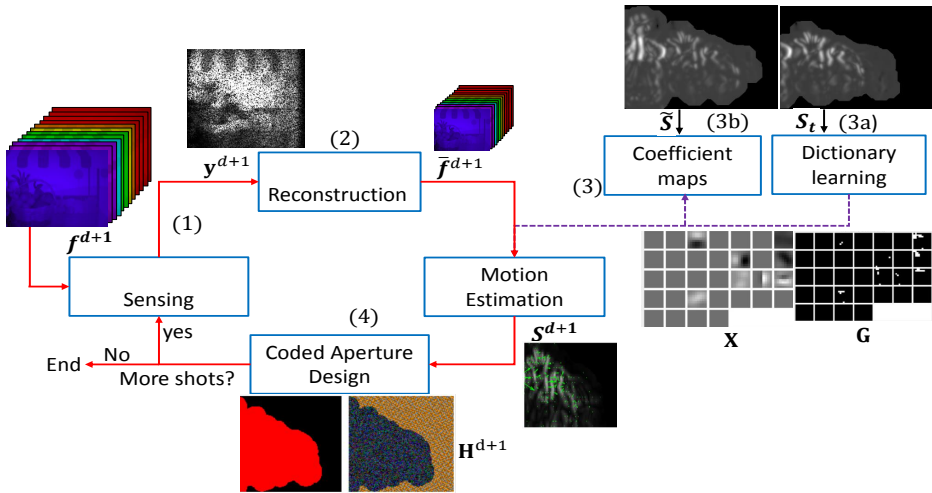
Random color aperture    Blue noise aperture<sup>1</sup>.

- Traditionally, coded apertures for video-CSI are designed randomly, ignoring the redundancy of the static and dynamic scene.
- Optimal approaches for sampling CSI could be extended to Video-CSI, however, those approaches promote complementary coded apertures, ignoring the motion between a couple of frames.

---

<sup>1</sup>Correa, Claudia, 2016 [1]

# Proposed Adaptive Coded Aperture Design



# Proposed Spectral Video Motion Estimation

- A pair of successive frames  $\mathbf{F}_H^{d-1}$  and  $\mathbf{F}_H^d$  (of  $\mathbb{R}^{M \times N \times L}$ ) from a spectral video acquired at time instants  $d - 1$  and  $d$
- Denote as  $\mathbf{S}_{(\ell,x)}^d$  and  $\mathbf{S}_{(\ell,y)}^d \in \mathbb{R}^{M \times N \times L}$  the video motions for the frame  $d$  along the  $x$  and  $y$  axes <sup>2</sup>.
- The motion estimation field is formulated as the minimization of a cost function with energy  $E_{\text{data}}(\mathbf{S}^d, \mathbf{F}_H^d, \mathbf{F}_H^{d-1})$  penalized by spatial and sparse regularizations, i.e.,

$$\underset{\mathbf{X}, \mathbf{S}^d}{\operatorname{argmin}} \left\{ E_{\text{data}}(\mathbf{S}^d, \mathbf{F}_H^d, \mathbf{F}_H^{d-1}) + \lambda_s E_{\text{spatial}}(\mathbf{S}^d) + \lambda_p E_{\text{sparse}}(\mathbf{S}^d, \mathbf{X}) \right\} \quad (1)$$

$\mathbf{F}^{d-1}$ spectral video sequence.	$\mathbf{F}^d$ spectral video sequence.	Horizontal motion $\mathbf{S}_{(\ell,x)}^d$ .	Vertical motion $\mathbf{S}_{(\ell,y)}^d$ .
---	---	--	--

<sup>2</sup>Note that the displacement vectors components along  $x$  and  $y$  are estimated independently for simplicity, i.e.,  $\mathbf{S}^d = \mathbf{S}_{(\ell,x)}^d$  or  $\mathbf{S}^d = \mathbf{S}_{(\ell,y)}^d$

# Data Fidelity and Spatial Regularization

Optical flow assumes brightness constancy and temporal consistency, leading to the following optical flow equation

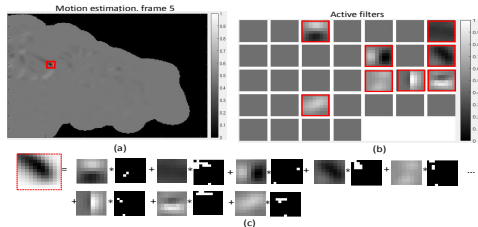
$$\partial_t \mathbf{f}_H^d + \nabla \mathbf{f}_H^T \mathbf{s}^d = 0 \quad (2)$$

where  $\mathbf{s}^d \in \mathbb{R}^{NM}$  represents the flow field such that  $\mathbf{s}_\ell^d$  is the vectorized video motion  $\mathbf{S}_\ell$ ,  $\partial_t \mathbf{f}_H^d$  denotes the temporal derivative and  $\nabla \mathbf{f}_H^T$  is the spatial gradient of the brightness. The data fidelity term resulting from optical flow is

$$E_{\text{data}}(\mathbf{s}^d, \mathbf{f}_H^d, \mathbf{f}_H^{d-1}) = \left\| \partial_t \mathbf{f}_H^d + \nabla \mathbf{f}_H^T \mathbf{s}^d \right\|_2^2 \quad (3)$$

where  $\|\cdot\|_2^2$  is the squared  $\ell_2$  norm. The first regularization term promotes smooth variations in the video motion field by using a standard total variation function,  $E_{\text{spatial}}(\mathbf{S}^d) = \|\nabla \mathbf{S}^d\|_2^2$

# Sparse Regularization Term



$\mathbf{S}^d$  is modeled as a convolution between the coefficient maps  $\mathbf{X}_v$  and a set of  $V$  filters  $\mathbf{G}_v$  [2],  
$$\mathbf{S}^d \approx \sum_{v=1}^V \mathbf{G}_v * \mathbf{X}_v$$

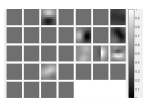
The second regularization term promotes sparsity of the motion vectors in a dictionary of representative motions. It decomposes the video motion  $\mathbf{S}^d$  as a convolution between  $V$  sparse coefficient maps  $\mathbf{X}_v$  and a set of  $V$  filters  $\mathbf{G}_v$ , i.e.,

$$E_{\text{sparse}}(\mathbf{S}^d, \mathbf{X}) = \left\| \mathbf{S}^d - \sum_{v=1}^V \mathbf{G}_v * \mathbf{X}_v \right\|_2^2 \quad (4)$$

where  $*$  denotes convolution.

# Dictionary Filters and Coefficients Maps

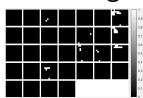
The dictionary learning is performed by solving the following problem (where  $\tilde{S}_d$  denotes the training video sequence which was obtained using Horn-Schunck optical flow estimation)



$$\operatorname{argmin}_{\mathbf{G}_v, \mathbf{X}_{d,v}} \frac{1}{2} \sum_d \left\| \sum_v \mathbf{X}_{d,v} * \mathbf{G}_v - \tilde{\mathbf{S}}^d \right\|_2^2 + \lambda \sum_{v=1}^V \sum_d \|\mathbf{X}_{d,v}\|_1 \quad (5)$$

s.t.       $\|\mathbf{G}_v\| = 1 \quad \forall v = 1, \dots, V.$

Once the dictionary  $\mathbf{G}_v$  has been determined, the coefficient maps of a sequence of test images denoted as  $\mathbf{S}_t^d$  are obtained by solving the following optimization problem



$$\operatorname{argmin}_{\mathbf{X}_v} \frac{1}{2} \left\| \sum_{v=1}^V \mathbf{X}_v * \mathbf{G}_v - \mathbf{S}_t^d \right\|_2^2 + \lambda \sum_{v=1}^V \|\mathbf{X}_v\|_1 \quad (6)$$

which can again be replicated using the ADMM algorithm.

# Spectral Video Motion Estimation

$$\begin{aligned} & \underset{\mathbf{S}_\ell^d}{\operatorname{argmin}} \left\{ E_{\text{data}}(\hat{\mathbf{F}}_H^{d-1}, \hat{\mathbf{F}}_H^d, \mathbf{S}_\ell^{d-1}) + \lambda_s \|\nabla \mathbf{S}_\ell^{d-1}\|_2^2 + \right. \\ & \left. \lambda_p(k) \|\mathbf{S}_\ell^{d-1} - \sum_v \mathbf{G}_v * \mathbf{X}_v\|_2^2 \right\} \text{ s.t. } \|\mathbf{G}_v\| = 1 \quad \forall v \end{aligned}$$

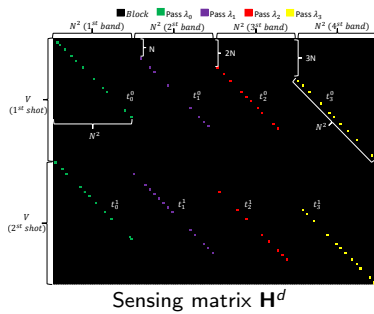
$\mathbf{f}^d = \Psi^d \boldsymbol{\theta}^d$  spectral video.      Horizontal motion  $\mathbf{S}_{(\ell,x)}^d$ .      Vertical motion  $\mathbf{S}_{(\ell,y)}^d$ .

# Compressive Spectral Video Sensing

$\mathbf{y}^d = \mathbf{H}^d \mathbf{f}^d$  Video spectral sequence.

Rows of  $\mathbf{H}^d$  represent the coded aperture.

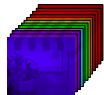
$\mathbf{f}^d = \Psi^d \theta^d$  Video spectral sequence.



# Low Resolution Reconstruction and Interpolation

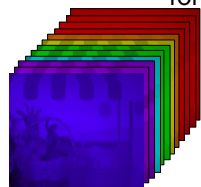
The low resolution datacube is computed by

$$\hat{\mathbf{f}}_L^{d-1} = \Psi_L^{-1}(\operatorname{argmin}_{\theta_L} \|\mathbf{y}^{d-1} - \mathbf{H}_L^{d-1} \Psi_L^{d-1} \theta_L^{d-1}\|_2^2 + \tau \|\theta_L^{d-1}\|_1)$$



$$\hat{\mathbf{f}}_L^d = \Psi_L^{-1}(\operatorname{argmin}_{\theta_L} \|\mathbf{y}^d - \mathbf{H}_L^d \Psi_L^d \theta_L^d\|_2^2 + \tau \|\theta_L^d\|_1)$$

where  $\mathbf{H}_L^0$  is the LR sensing matrix,  $\Psi_L^d$  is the LR representation basis, and  $\theta_L^d$  is the vectorization of a sparse vector for the LR reconstruction.



The LR datacube is interpolated using  $P(\cdot)$  a bilinear interpolator  $\hat{\mathbf{f}}_H^{d-1} \leftarrow \mathbf{P}(\hat{\mathbf{f}}_L^{d-1})$ , and  $\hat{\mathbf{f}}_H^d \leftarrow \mathbf{P}(\hat{\mathbf{f}}_L^d)$ .

# Design of Video Adaptive Colored Coded Aperture (VA-CCA)

$$\text{Motion estimation} \\ \sqrt{(\mathbf{S}_{(\ell,x)}^d)^2 + (\mathbf{S}_{(\ell,y)}^d)^2}.$$

$$\text{Thresholding} \\ \mathbf{Q}_\ell^d \leftarrow (\mathbf{S}_\ell^{d-1}, \mathbf{S}_\ell^d)$$

$$\text{Next coded aperture} \\ \mathbf{r}_\ell^d \leftarrow \mathbf{q}_\ell^d \odot \mathbf{b}_\ell^d + (1 - \mathbf{q}_\ell^d) \odot \hat{\mathbf{b}}_\ell^d$$

# Simulation Parameters

Training spectral motion sequence  $\tilde{\mathbf{S}}^d$

Test spectral motion sequence  $\mathbf{S}_t^d$

Step	Parameters	Values
Dictionary learning	Database 23 frames	Peasant woman 1 [3]
	Filter size	$8 \times 8$
	Filters number	$M = 32$
	Sparsity term	$\lambda = 0.05$
	Number of iteration	500
Sparse coding	Database 23 frames	Peasant woman 2 [3]
	Number of iteration	500
Video motion estimation	Regularization parameter	$\lambda_s = 0.75$
	Sparsity term (video)	$\lambda_d = \{1 \times 10^{-6} \times 10^{-3}\}$

# Comparison of Quality of Image Reconstruction

Average PSNR=20.4296 dB. Average PSNR=21.1145 dB. Average PSNR=19.6498 dB. Average PSNR=18.7091dB.

Blue noise non adaptive  
(BNA).

Video colored coded aperture  
(V-CCA).

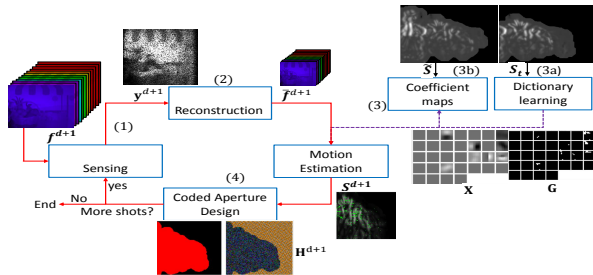
Random colored coded  
aperture (R-CCA).

Block-unblock coded aperture  
(BUA).

Size of  $\mathbf{F}^d \in \mathbb{R}^{128 \times 128 \times 12}$  and 23 frames.

# Conclusions

- A new design of adaptive colored coded apertures (VA-CCA) for spectral video.
- The approach provides a motion estimation between frames to sample the static and the dynamic scene differently.
- The proposed approach overcomes, block-unblock CA (2.4 dB), random-colored CA (1.46 dB), non-adaptive blue noise (0.68 dB).



# Questions?



# References

-  C. V. Correa, H. Arguello, and G. R. Arce, "Spatiotemporal blue noise coded aperture design for multi-shot compressive spectral imaging," *J. Opt. Soc. Am. A*, vol. 33, no. 12, pp. 2312–2322, Dec 2016. [Online]. Available: <http://josaa.osa.org/abstract.cfm?URI=josaa-33-12-2312>
-  B. Wohlberg, "Efficient algorithms for convolutional sparse representations," *IEEE Trans. Image Process.*, vol. 25, no. 1, pp. 301–315, Jan 2016.
-  K. M. León-López, L. V. Galvis Carreño, and H. Arguello Fuentes, "Temporal colored coded aperture design in compressive spectral video sensing," *IEEE Transactions on Image Processing*, vol. 28, no. 1, pp. 253–264, Jan 2019.

# Video Motion Estimation Algorithm (Initialization)

**Input:**  $\lambda_s, \lambda_p, K, D, \lambda, \rho, \tilde{\mathbf{S}}, \mathbf{S}_t$  : Training/test video motions

**Output:**  $\mathbf{S}_\ell^d$

- 1: **function** CODED APERTURE DESIGN USING VIDEO MOTION ESTIMATION ( $\mathbf{y}^0, \mathbf{y}^1, \lambda_s, \lambda_p, K, J, \lambda, \rho, \tilde{\mathbf{S}}, \mathbf{S}_t$ )
- 2:    $\mathbf{G}_v \leftarrow$  Computes the dictionary by solving (5)
- 3:    $\mathbf{X}_v \leftarrow$  Computes the coefficient maps by solving (6)
- 4:    $\mathbf{y}^0 \leftarrow \mathbf{H}^0 \mathbf{f}$     ▷ First snapshot
- 5:    $\hat{\mathbf{f}}_L^0 \leftarrow \Psi_L^{-1}(\operatorname{argmin}_{\boldsymbol{\theta}_L} \|\mathbf{y}^0 - \mathbf{H}_L^0 \Psi_L^d \boldsymbol{\theta}_L^d\|_2^2 + \tau \|\boldsymbol{\theta}_L^d\|_1)$
- 6:    ▷ Low-resolution
- 7:    $\hat{\mathbf{f}}_H^0 \leftarrow \mathbf{P}(\hat{\mathbf{f}}_L^0)$     ▷ Interpolation
- 8:    $\hat{\mathbf{F}}_H^0 \leftarrow \text{rearrange}(\hat{\mathbf{f}}_H^0)$     ▷ Rearrange
- 9:    $\hat{\mathbf{f}} \leftarrow \Psi^{-1}(\operatorname{argmin}_{\boldsymbol{\theta}} \|\mathbf{y} - \mathbf{H} \Psi \boldsymbol{\theta}\|_2^2 + \tau \|\boldsymbol{\theta}\|_1)$
- 10:   **Motion estimation and Adaptive Coded Aperture Desing**
- 11:   **return**  $\mathbf{S}_\ell^d$     ▷ (Estimated motion field)

# Motion estimation and Adaptive Coded Aperture Design

```
1: for  $k \leftarrow 1, K$  do
2:   for  $d \leftarrow 1, D$  do
3:      $\hat{\mathbf{f}}_L^d \leftarrow \Psi_L^{-1}(\operatorname{argmin}_{\theta_L} \|\mathbf{y}^d - \mathbf{H}_L^d \Psi_L^d \theta_L^d\|_2^2 + \tau \|\theta_L^d\|_1)$ 
4:   end for
5:    $\hat{\mathbf{f}}_H^d \leftarrow \mathbf{P}(\hat{\mathbf{f}}_L^d)$  ▷ Low-resolution
6:    $\hat{\mathbf{F}}_H^d \leftarrow \text{rearrange}(\hat{\mathbf{f}}_H^d)$  ▷ Interpolation
7:   for  $\ell \leftarrow 1, L$  do
8:      $\operatorname{argmin}_{\mathbf{S}_\ell^d} \{ E_{\text{data}}(\hat{\mathbf{F}}_H^{d-1}, \hat{\mathbf{F}}_H^d, \mathbf{S}_\ell^{d-1}) +$  ▷ Rearrange
9:        $\lambda_s \|\nabla \mathbf{S}_\ell^{d-1}\|_2^2 + \lambda_p(k) \|\mathbf{S}_\ell^{d-1} - \sum_v \mathbf{G}_v * \mathbf{X}_v\|_2^2 \}$ 
10:      s.t.  $\|\mathbf{G}_v\| = 1 \forall v$  ▷ Video motion estimation
11:       $\mathbf{Q}_\ell^d \leftarrow (\mathbf{S}_\ell^{d-1}, \mathbf{S}_\ell^d)$  ▷ Thresholding motion
12:       $\mathbf{q}_\ell^d \leftarrow \text{vec}(\mathbf{Q}_\ell^d)$  ▷ Vectorized motion areas
13:       $\mathbf{r}_\ell^d \leftarrow \mathbf{q}_\ell^d \odot \mathbf{b}_\ell^d + (1 - \mathbf{q}_\ell^d) \odot \hat{\mathbf{b}}_\ell^d$  ▷ Next code
14:       $\mathbf{H}_\ell^d \leftarrow \text{rearrange}(\mathbf{r}_\ell^d)$  ▷ Rearrange
15:       $\mathbf{y}^d \leftarrow \mathbf{H}^d \mathbf{f}$  ▷ Next snapshot
```

## Parameters $\lambda$ and $\rho$

	$\rho_0 = 25$	$\rho_1 = 50$	$\rho_2 = 100$	$\rho_3 = 150$
$\lambda_0 = 0.0005$	30.9600	30.8260	30.7236	31.1311
$\lambda_1 = 0.0001$	38.1156	37.7255	38.6955	39.9385
$\lambda_2 = 0.00005$	33.5062	32.0604	<b>40.3777</b>	38.4921
$\lambda_3 = 0.00001$	29.6564	30.5600	30.0820	29.5902
$\lambda_4 = 0.000001$	34.5530	28.1833	33.5431	30.4982

**Table 1:** Image quality (PSNR) with 100 iteration of (CBPDN) for different choices of  $\lambda$  and  $\rho$  by using the motion horizontal ground-truth.

	$\rho_0 = 25$	$\rho_1 = 50$	$\rho_2 = 100$	$\rho_3 = 150$
$\lambda_0 = 0.0005$	37.7552	38.2876	38.5107	38.6064
$\lambda_1 = 0.0001$	41.3404	39.6111	39.7874	40.1052
$\lambda_2 = 0.00005$	41.6682	39.8263	40.6523	42.0653
$\lambda_3 = 0.00001$	42.1040	39.8192	40.1028	<b>49.2796</b>
$\lambda_4 = 0.000001$	41.0436	39.6918	40.9101	38.4830

Image quality (PSNR) with 100 iteration of (CBPDN) for different choices of  $\lambda$  and  $\rho$  by using the motion vertical ground-truth.